Transactions of the Korean Nuclear Society Spring Meeting
Jeju, Korea, May 22-23, 2025

Progress in development of soft X-ray array in KSTAR by multichannel SiPM readout of a scintillator

M. W. Lee [a], Junghee Kim [b], D. H. Kim [a], C. Sung [a*]
[a]*Department of Nuclear and Quantum Engineering, Korea Advanced Institute of Science and Technology, Daejeon 34141, Republic of Korea*
[b]*Korea Institute of Fusion Energy, Daejeon 34133, Republic of Korea*
[*]*Corresponding author: choongkisung@kaist.ac.kr*

*Keywords: Soft X-ray, Scintillator, SiPM, PMT, KSTAR

1. Introduction

Soft X-ray (SXR) diagnostics are widely utilized for studying the magnetohydrodynamic activities of fusion plasma [1,2], as they offer high temporal resolution and non-invasive measurement capabilities. In Korea Superconducting Tokamak Advanced Research (KSTAR), we have been developing SXR diagnostics based on optical systems with scintillators for high radiation hardness [3]. In the early stage of the development, we used photomultiplier tube (PMT) to measure the light signals from scintillator. However, the scalability of PMT is limited by its high cost for multichannel application. Additionally, unlike PMT, SiPM is not affected by magnetic fields, making it more suitable for the Tokamak environment. Therefore, we try to apply silicon photomultiplier (SiPM) to build the multichannel scintillator readout. In this paper, we present the progress in the development of a SXR diagnostic in KSTAR.

2. Methods and Results

2.1 SXR Measurement System

The KSTAR SXR system [4] consists of pinhole cameras equipped with scintillator receivers. The SXR camera was installed at the N-port of KSTAR, with its schematic illustrated in Fig. 1. In addition to the SXR intensity, the KSTAR SXR system is capable of measuring electron temperature through two-filter method [5]. Therefore, each receiver assembly contains 32 channels with two scintillators and filters (Beryllium 10 μm and 50 μm), having overlapped 16 lines of sight (LOS) in the poloidal plane.

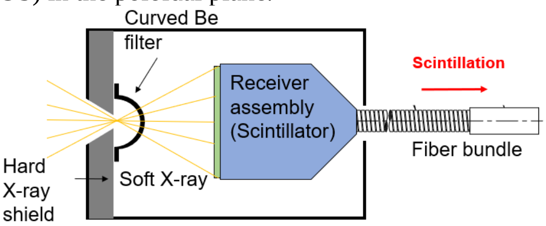

Fig. 1 Schematic of the soft X-ray camera

To achieve higher temporal resolution, a YAG:Ce scintillator (35 μm thickness) with a decay rate of 70 ns was used. The scintillations generated by incident SXR radiation are collected by a lens array (diameter of 3 mm), each corresponding to a measurement channel. The collected light signals are transmitted outside the vacuum vessel through an optical fiber bundle and detected by photosensors such as PMTs and SiPMs.

In this study, we initially developed a SiPM readout system using a single-channel SiPM before moving on to the multichannel system. The schematic of the SiPM readout is shown in Fig. 2(a). For the SiPM, we selected the RGB-type (Red-Green-Blue) model (ASD-RGB4S-P) from AdvanSid to align its sensitivity with the emission peak of YAG:Ce, as depicted in Fig. 2(b). One RGB SiPM chip has 4×4 mm^2 effective active area with cell size of 40 μm × 40 μm (total 9340 cell count).

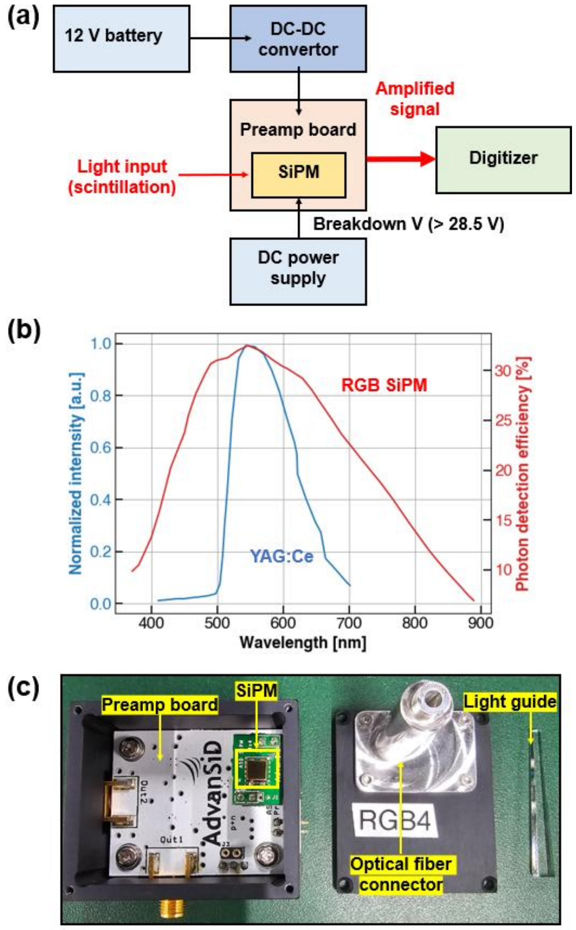

Fig. 2 (a) Block diagram of the SiPM readout system. (b) Normalized intensity of the YAG:Ce scintillator over wavelength. The photon detection efficiency of the RGB type SiPM is also shown. (c) A picture of SiPM, preamp board, and housing.

The chip is mounted on a socket and connected to evaluation board (ASD-EP-EB-PZ), which is a signal amplifier with transimpedance gain of 100 Ω. The breakdown voltage is around 28.5 V, so we connected a DC power supply as shown in Fig. 2(a). To activate the amplifier, we used 12 V battery and DC-DC convertor that supply ±5 V. The amplified signals through the preamp board are read by a digitizer.

For the mechanical structures of the SiPM system, we made a metal housing that encloses the SiPM and preamp board to block the possible stray light. Figure 2(c) shows the components of the SiPM system including the SiPM chip, preamp board, and metal housing. On the top of the housing, we put a light guide that connects the SiPM and optical fiber interface. The light signals from the optical fiber (with a diameter of 0.6 mm) are spread into a 4×4 mm² shape when passing through the light guide. This helps prevent signal saturation at the SiPM by ensuring uniform illumination of the input light across the SiPM microcells. Figure 3 shows the picture of whole SiPM assemblies that were used for measurements. We made four single-channel SiPM systems for KSTAR measurements.

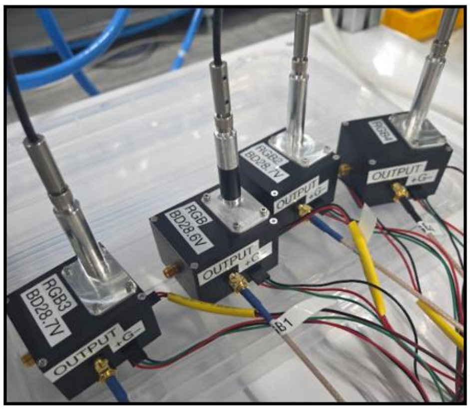

Fig. 3 Picture of the single-channel SiPM modules. The optical fibers were connected to SiPM chip through light guides.

2.2 Preliminary Results of KSTAR discharges

During the 2024 KSTAR campaign, we tested the SiPM systems and compared their performance with previous PMT data. The data from discharge #33667, obtained during the 2023 campaign, were collected using PMTs, as shown in Fig. 4(a). These signals were measured with a commercial PMT module (Hamamatsu H10723-210) and a variable gain preamplifier (FEMTO DHPCA-100). In Fig. 4(b), the SiPM data of discharge #36188 were multiplied by a factor of 100 to compensate for the fixed transimpedance gain of the current SiPM module. While the PMT system had a variable gain of 10^4 V/A, the SiPM module had a fixed gain of 10^2 V/A. The 2024 campaign results, which showed comparable SXR signal levels between the SiPM and PMT systems once the transimpedance gain was compensated, confirmed that the SiPM can be utilized for KSTAR SXR measurements as a replacement for the previous PMT modules. In addition, these results also indicate that increasing a preamplifier gain for the SiPM system will be necessary for its multichannel version.

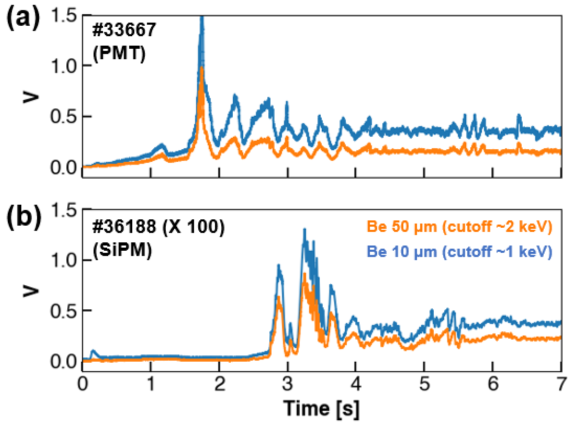

Fig. 4. SXR data of KSTAR discharge #33667 and #36188 using different Be filters. Both cases show the increase of signals after high confinement mode (H-mode) transition around 2~3 seconds. (a) PMT and (b) SiPM data. All sight line crossed R ~ 1.9 m at Z=0. The cutoff energy of the filter is point of 50% transmission.

We also designed the multichannel SiPM readout based on single-channel results. For multichannel applications, we developed a 4 × 4 SiPM array along with a custom 16-channel preamplifier system. Figure 5 shows the assembly of 16-channel fiber bundle and SiPM. The fiber array in Fig. 5(a) has the same spacing with the SiPM array in Fig. 5(b). The fiber array and SiPM are connected through the holder that has light guides, as shown in Fig. 5(c). For KSTAR N-port array, we planned to make total 64 channels using the SiPM arrays. By the end of the 2024 KSTAR campaign, the entire system including fiber bundles, the SiPM array, and preamp systems, was installed at KSTAR. However, due to a malfunction in the multichannel digitizer, we were unable to test the complete system. Full-channel measurements are planned for the upcoming 2025 campaign, followed by further tests and channel calibrations to optimize system performance.

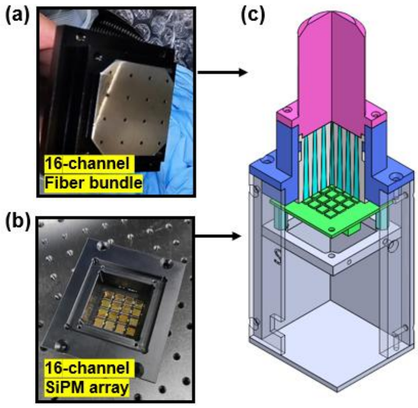

Fig. 5. Pictures of the 16-channel (a) fiber bundle and (b) SiPM array. (c) The assembly of fiber bundle and SiPM array

3. Conclusions

We developed a soft X-ray measurement system using SiPM and installed it at KSTAR. The system consists of an SXR receiver with scintillators, fiber optics, and a multichannel SiPM readout. Initial measurements with four single-channel SiPM modules were done during the 2024 KSTAR campaign. The results confirmed that the SiPM system can measure the KSTAR SXR, replacing the PMTs that need high cost for multichannel application. Based on the single-channel results, we also designed a multichannel SiPM array. Further optimization of the multichannel system is needed to ensure reliable measurements, which will be addressed in the upcoming 2025 KSTAR campaign.

Acknowledgments

This research was supported by R&D Program of "High Performance Tokamak Plasma Research & Development (code No. EN2501)" through the Korea Institute of Fusion Energy (KFE) and National Research Foundation of Korea (NRF) funded by the Ministry of Science and ICT of the Republic of Korea (RS-2022 00155956).

REFERENCES

[1] L. Delgado-Aparicio et al., Plasma Phys. Control. Fusion. 53 (2011) 035005.
[2] C. Brandt et al., Plasma Phys. Control. Fusion. 62 (2020) 035010.
[3] L. F. Delgado-Aparicio et al., Appl. Opt. 46 (2007) 6069-6075.
[4] M. W. Lee et al., Rev. Sci. Instrum., 94 (2023) 053507.
[5] Delgado-Aparicio et al., Plasma Phys. Control. Fusion 2007, 49, 1245–1257.